# Ag-Cu catalysts for ethylene epoxidation: Selectivity and activity descriptors

Ngoc Linh Nguyen, Stefano de Gironcoli, and Simone Piccinin

Citation: The Journal of Chemical Physics **138**, 184707 (2013); doi: 10.1063/1.4803157
View online: http://dx.doi.org/10.1063/1.4803157
View Table of Contents: http://scitation.aip.org/content/aip/journal/jcp/138/18?ver=pdfcov
Published by the AIP Publishing

# Ag-Cu catalysts for ethylene epoxidation: Selectivity and activity descriptors

Ngoc Linh Nguyen,[1] Stefano de Gironcoli,[1,2] and Simone Piccinin[1,2,a)]
[1]*Scuola Internazionale Superiore di Studi Avanzati (SISSA), via Bonomea 265, I-34136 Trieste, Italy*
[2]*CNR-IOM Democritos, via Bonomea 265, I-34136 Trieste, Italy*

(Received 13 March 2013; accepted 16 April 2013; published online 10 May 2013)

Ag-Cu alloy catalysts for ethylene epoxidation have been shown to yield higher selectivity towards ethylene oxide compared to pure Ag, the unique catalyst employed in the industrial process. Previous studies showed that under oxidizing conditions Cu forms oxide layers on top of Ag. Using first-principles atomistic simulations based on density functional theory, we investigate the reaction mechanism on the thin oxide layer structures and establish the reasons for the improved selectivity. We extend the range of applicability of the selectivity descriptor proposed by Kokalj *et al.* [J. Catal. **254**, 304 (2008)], based on binding energies of reactants, intermediates, and products, by refitting its parameters so as to include thin oxide layer catalysts. We show that the selectivity is mainly controlled by the relative strength of the metal-carbon vs. metal-oxygen bonds, while the height of the reaction barriers mostly depend on the binding energy of the common oxametallacycle intermediate.
 [http://dx.doi.org/10.1063/1.4803157]

## I. INTRODUCTION

The production of ethylene oxide (EO) through the partial oxidation of ethylene is one of the largest industrial catalytic processes,[1] with a world annual production of about 19 million metric tons in 2009.[2] Ethylene oxide is mostly used in the synthesis of ethylene glycol, an important chemical for the production of antifreeze, polyester, and polyethylene terephthalate (PET). EO finds applications also in the production of surfactants and detergents. The oxidation process must be carried out with high selectivity, since the competing reaction, leading to total combustion ($CO_2 + H_2O$) is thermodynamically favored. The unique catalyst used in the industry is Ag, in the form of particles dispersed on an $\alpha$-$Al_2O_3$ support.[3] While pure Ag achieves selectivities towards the formation of EO lower than 50%, the addition of suitable promoters (typically Cl and Cs) can enhance the selectivity up to around 90%.[4]

The nature of the oxygen species on Ag is responsible for the epoxidation of ethylene and the reasons why silver is the unique catalyst for this process have long been debated.[5–14] Of the various O species identified on Ag, a so called "electrophilic" oxygen is believed to be responsible for the insertion into the electron-rich C=C double bond of ethylene, while the "nucleophilic" oxygen should activate the C–H bond in ethylene, the first step towards total combustion.[12] The former type of oxygen is usually identified as a form of atomic oxygen chemisorbed on clean Ag, but recent theoretical works point towards a 2-fold coordinated oxygen atom at the surface of $Ag_2O(001)$,[15] while the latter is thought to be an oxygen atom at the surface of oxide-like layer.[12,16] Moreover, on Ag oxygen can diffuse into the subsurface layers,[12,17–19] and several works stressed the key role played by subsurface oxygen in this catalytic process.[7–9]

On silver surfaces, experimental and theoretical works by Linic and Barteau[20,21] suggest the reaction mechanism to involve a common oxametallacycle (OMC) intermediate for both the selective path leading to EO and for the unselective path leading to acetaldehyde (Ac), which is quickly converted to $CO_2$ on Ag surfaces. On $Ag_2O(001)$, on the other hand, van Santen and co-workers identified competing a mechanism, where EO forms via a non-activated direct path without involving any intermediate.[15] When considering other coinage metals, theoretical calculations show that the Cu(111) surface can, in principle, afford even higher selectivities than Ag.[22,23] The unique ability of Ag to selectively catalyze this reaction has been attributed to Ag being able to bind oxygen strongly enough to dissociate $O_2$, but not too strongly so as to make desorption of EO more activated than competing paths leading to total oxidation.[14]

Given the industrial relevance of ethylene epoxidation, modifications of the Ag surface to improve the selectivity towards the formation of EO have long been attempted. Barteau and co-workers, in particular, through a combination of theoretical modeling and experiments on model catalysts, have shown that alloying Ag with Cu significantly improves the selectivity compared to pure Ag.[24] This improvement was rationalized on the basis of the formation of a surface alloy.[24] At temperature and pressure typically used in industrial production of ethylene oxide ($T \simeq 500$–$600$ K, $p \simeq 1$–$10$ atm), however, Cu impurities in Ag tend to segregate to the surface and form copper oxide.[26] Cupric oxide, CuO, is the thermodynamically stable form of copper oxide at these conditions of temperature and pressure. *In situ* XPS measurements show that both Cu(I) and Cu(II) are present at the surface of Ag-Cu alloys at 520 K and a pressure of 0.5 mbar.[25] These measurements reveal the presence of thin overlayers on top of silver

a)Electronic mail: piccinin@sissa.it

 

particles where Cu is present in its oxidized form, while no signatures of metallic Cu are detected. This is in agreement with theoretical studies indicating a thermodynamic driving force towards the formation of thin copper oxide structures, and showing that a variety of surface structures with different stoichiometries can form under these conditions, all having similar surface energies.[25–29]

While previous studies focused on the structure of Ag-Cu alloys under reaction conditions, the crucial issue of how (oxidized) Cu alloyed into Ag improves the catalytic properties of pure Ag is still unclear. In this work, we employ density functional theory (DFT) calculations to model the mechanism of ethylene epoxidation promoted by thin Cu-oxide layers on Ag surfaces. We investigate, in particular, the role of sub-surface oxygen and compare the results obtained for the alloy to the case of pure Ag. We develop an indicator of the catalysts activity and selectivity based on the binding energy of the reaction intermediates, along the lines proposed by Kokalj *et al.*,[30] that enables us to rationalize the catalytic properties of Cu-oxide overlayers on Ag. We show that thin Cu-oxide layers improve the selectivity towards EO compared to pure Ag due to an increase of the metal-oxygen bond relative to the metal-carbon bond, in agreement with what has been proposed for clean metal surfaces.[30]

## II. METHODS

In this work, the DFT calculations are performed using the generalized gradient approximation (GGA) of Perdew-Burke-Ernzerhof (PBE)[31] for the exchange and correlation functional. The electron-ion interactions are computed using ultrasoft pseudopotentials,[32,33] including scalar relativistic effects, and the energy cutoff for the plane wave expansion is 30 Ry (300 Ry for the charge density cutoff). Brillouin-zone integration has been performed with the special-point technique,[34] and broadening the Fermi surface according to the Marzari-Vanderbilt cold-smearing technique,[35] using a smearing parameter of 0.03 Ry (0.41 eV). We model the catalysts employing a periodically repeated slab geometry using a (2 × 2) surface supercell for the (111) surface orientation, with adsorbates on one side of the slab only. The Brillouin-zone integrations are performed with a 6 × 6 × 1 Monkhorst-Pack grid.[34] The Ag slabs are four layers thick and the bottom two layers are kept fixed in their bulk positions during relaxations. A 12 Å vacuum layer is used, which is found to be sufficient to ensure negligible coupling between periodic replicas of the slab.

For the calculation of the reaction pathways we adopt the nudged elastic band (NEB) technique.[36] The transition state along the minimum energy path is located using the climbing image method.[36] During the NEB minimization, all the atoms except the bottom two layers of the silver slab are allowed to relax, until the forces are less than 0.05 eV/Å. All the calculations are performed using the PWscf code contained in the Quantum-ESPRESSO distribution.[37]

To take into account the effects of temperature ($T$) and pressure ($p$) of reactive environment, we use the constrained *ab initio* atomistic thermodynamics approach,[19,38,39] in which the system under investigation is considered to be in contact with the oxygen and ethylene reservoirs at fixed chemical potentials (i.e., at fixed temperature and partial pressure), while the two reservoirs do not interact with each other. We define the surface free energy of adsorption as

$$\gamma(T) = \left(E_{\text{tot}} - E_{\text{Ag}}^{\text{slab}} - N_{\text{Ag}}\mu_{\text{Ag}} - N_{\text{Cu}}\mu_{\text{Cu}}, \right. \quad (1)$$

$$\left. - N_{\text{O}}\mu_{\text{O}} - N_{\text{C}_2\text{H}_4}\mu_{\text{C}_2\text{H}_4}\right)/A, \quad (2)$$

where $A$ is the surface area, $E_{\text{tot}}$ is the total energy of system, $E_{\text{Ag}}^{\text{slab}}$ is the total energy of the Ag slab, $N_{\text{Ag}}$ is the number of Ag atoms in addition to the ones contained in the slab, $N_{\text{Cu}}$, $N_{\text{O}}$, and $N_{\text{C}_2\text{H}_4}$ are number of Cu and O atoms, and $C_2H_4$ molecule, respectively. $\mu_{\text{Ag}}$, $\mu_{\text{Cu}}$, $\mu_{\text{O}}$, and $\mu_{\text{C}_2\text{H}_4}$ are the chemical potential of Ag, Cu, O, and $C_2H_4$, respectively. In this expression, the free energies of the adsorption system and the clean slab are approximated with total energies, thus neglecting vibrational and configurational entropy terms. With this definition, lower values of surface free energy correspond to more stable structures. The chemical potentials of Ag and Cu are fixed at their bulk values, while the oxygen and ethylene chemical potentials depend on temperature and pressure. The detailed determination of these chemical potentials can be found in Ref. 29.

## III. RESULTS AND DISCUSSION

In our previous works[25–29,40] we have shown, theoretically and experimentally, that under conditions of temperature and pressure relevant for ethylene epoxidation, copper in Ag-Cu alloys tends to segregate to the surface and form thin oxide layers. While we theoretically identified several candidate surface structures with similar energetics, here we will focus on the (111) facet and in particular on the "CuO/Ag(111)" structure, consisting of an overlayer with a one-to-one ratio of Cu and O in a (2 × 2) unit cell on top of a Ag(111) slab. This single "CuO" layer bears little structural resemblance to the corresponding CuO bulk oxide.[26] Moreover, we stress that DFT-PBE fails to accurately describe the electronic structure of bulk CuO, predicting this material to be a metal with an almost orthorhombic structure, rather than an antiferromagnetic semiconductor with a monoclinic structure.[41] Therefore, when considering the formation of thicker CuO layers, we must keep in mind that absolute values of quantities such as the surface free energy are likely affected by a significant error. We will first examine the role of sub-surface oxygen in the catalytic properties of this structure, and compare the results with Ag(111) and with structures in which the Cu substitutes for Ag in CuO/Ag(111). This will enable us to build indicators of activity and selectivity that will be instrumental for rationalizing the improvement of selectivity due to the formation of a CuO layer on Ag(111).

### A. Thermodynamic stability of $O^{sub}$ in Ag-Cu alloys

The role played by subsurface oxygen ($O^{sub}$) in ethylene epoxidation has been investigated for more than 30 years, but is still a controversial topic. van Santen *et al.* have shown that $O^{sub}$ acts as a promoter that can improve selectivity of Ag. $O^{sub}$ is proposed to reduce the strength of

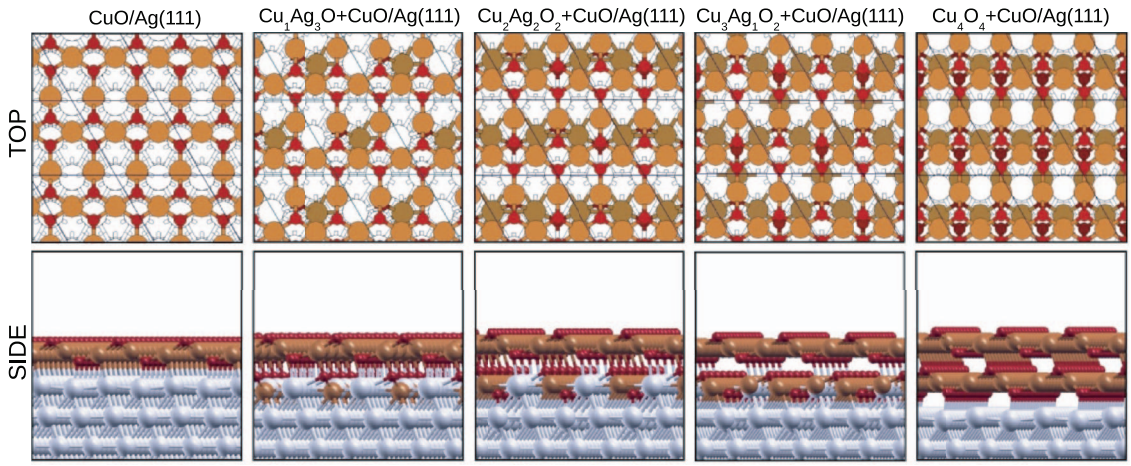


FIG. 1. The top-view (top panel) and side-view (bottom panel) of the most stable structures at the given Cu surface content. In the top panel, the small red atoms represent oxygen on the first thin oxide layer, the large light-brown ones represent copper on the first thin oxide layer, the small dark-red ones represent sub-surface oxygen, the large dark-brown ones represent copper on the second layers, and the large white ones represent silver.

the bonds of on-surface oxygen, thus facilitating the binding of on-surface oxygen to the C=C double bond of ethylene, forming EO.[9] Mavrikakis *et al.*, on the other hand, through DFT calculations, found that $O^{sub}$ can stabilize the on-surface oxygen,[19,42,43] and also increases the chemisorption energy of ethylene on pure Ag surface.[42] Experiments on ethylene epoxidation on pure Ag surfaces detected the presence of $O^{sub}$ upon oxidizing ethylene molecules. Nevertheless, the catalytic promotion of this oxygen strongly depends on the experimental set-up. For example, in the transient experiments by Grant and Lambert[7] and van Santen and co-workers,[8,44] an increase of silver selectivity towards the formation of EO was found to correlate with presence of $O^{sub}$. On the other hand, experiments done by Campbell and co-workers, under steady-state conditions, showed that as the temperature increases oxygen tends to be incorporated in subsurface positions, but this does not seem to effect the catalytic properties of the system.[5,6] By using temperature programmed reaction (TPR) and temperature programmed desorption (TPD) for ethylene and oxygen species, Atkins *et al.* showed that $O^{sub}$ can be present on Ag(111) surface in an amount up to 2.28 ML.[45] Moreover, measurements of Ag surfaces in oxygen atmosphere showed that $O^{sub}$ induces an electronic effect on Ag atoms on surfaces in the same way as Cl does.[46–48]

In this work we examine a variety of structures containing subsurface oxygen. For the clean Ag(111) surface, we consider a (2 × 2) unit cell with 0.25 ML coverage of chemisorbed atomic oxygen on the surface. In agreement with Li *et al.*,[19] we find two stable configurations for $O^{sub}$ having nearly identical surface free energy: (i) a structure with the surface oxygen at a fcc site and $O^{sub}$ at a tetrahedral (tetra) subsurface site, denoted as $O^{sub}$(tetra) + O(fcc)/Ag(111), and (ii) a structure with the surface oxygen at a hcp site and $O^{sub}$ at a octahedral (octa) site, denoted as $O^{sub}$(octa) + O(hpc)/Ag(111).

In the case of the CuO/Ag(111) structure, we find the most stable site for $O^{sub}$ to be at the interface between the Cu-oxide layer and the Ag slab, corresponding to a fcc adsorption site of the underlying Ag(111) surface. However, as previously discussed,[29] the formation of $O^{sub}$ at temperature and pressure relevant for ethylene epoxidation is not thermodynamically favorable. We therefore considered the effect of substituting Ag with Cu in the first Ag layer of the CuO/Ag(111) structure. We label these structures $Cu_xAg_{(4-x)}O_y$ + CuO/Ag(111), where $x$ is the number of Cu atoms replacing Ag and $y$ is the number of O atoms at subsurface positions. The $Cu_4O_4$ + CuO/Ag(111) thus corresponds to two layers of CuO on Ag(111) (see Fig. 1). $O^{sub}$ in this case can be seen as playing the role of the nucleation site for bulk oxide formation.[19] In recent studies of oxidation reactions over transition metal such as Ru, Rh, Ag, and alloy surfaces such as NiAl(110),[19,49–51] it has been shown that the incorporation of oxygen into subsurface sites is a precursor to the oxide formation.[19,52]

In Fig. 2, we present the surface free energy (Eq. (1)) of the $Cu_xAg_{(4-x)}O_y$ + CuO/Ag(111) structures at the oxygen chemical potential $\mu_O = 0.61$ eV (corresponding to $p(O_2)$ = 1 atm and $T$ = 600 K), as a function of the Cu content. Correspondingly, the content of subsurface oxygen is varied between 0 and 1 ML. In the case of Cu content equal to 1 ML (i.e., no Cu replacing Ag in the second layer) the presence of $O^{sub}$ is unfavorable. At least a quarter of a monolayer of Cu in the second layer (i.e., one Cu replacing an Ag atom in the

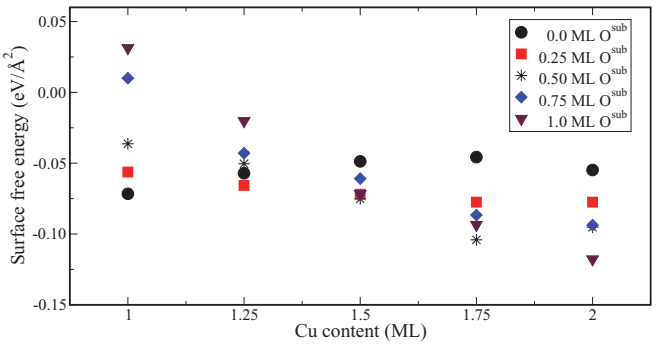


FIG. 2. Surface phase diagram showing the surface free energy at $\Delta\mu_O$ = −0.61 eV ($T$ = 600 K, $p_O$ = 1 atm), for the structures as the function of Cu surface content, while changing the $O^{sub}$ coverage.

TABLE I. For all the structures considered in this work we report coverages of Cu and O (in ML), activation energies and their difference ($\Delta E^*$) computed using NEB, binding energies of the OMC intermediate, O, $CH_3$, and $CH_3O$ radicals, and the final products Ac and EO. The last column shows the value of the selectivity indicator ($\Delta E^{*(SI)}$). All energies are in eV. The (a) and (b) superscripts refer to two different geometries for the OMC intermediate.

| Surface structure | $\Theta_{Cu}$ | $\Theta_O$ | $E^*_{Ac}$ | $E^*_{EO}$ | $\Delta E^*$ | $E^b_{OMC}$ | $E^b_O$ | $E^b_{CH_3}$ | $E^b_{CH_3O}$ | $E^b_{Ac}$ | $E^b_{EO}$ | $\Delta E^{*(SI)}$ |
|---|---|---|---|---|---|---|---|---|---|---|---|---|
| O(fcc)Ag(111) | 0.00 | 0.00 | 0.64 | 0.72 | −0.08 | 0.24 | −0.40 | −1.59 | −2.17 | −0.13 | −0.06 | −0.03 |
| $O^{sub}$(tetra)+O(fcc)/Ag(111)[a] | 0.00 | 0.25 | 0.63 | 0.88 | −0.25 | −0.06 | −0.95 | −1.98 | −2.38 | −0.19 | 0.01 | −0.15 |
| $O^{sub}$(tetra)+O(fcc)/Ag(111)[b] | 0.00 | 0.25 | 1.20 | 1.32 | −0.12 | −0.58 | −0.95 | −2.32 | −2.51 | −0.41 | −0.26 | −0.15 |
| $O^{sub}$(octa)+O(hpc)/Ag(111)[a] | 0.00 | 0.25 | 0.77 | 1.01 | −0.24 | 0.15 | −0.80 | −1.69 | −2.10 | −0.12 | −0.06 | −0.10 |
| $O^{sub}$(octa)+O(hpc)/Ag(111)[b] | 0.00 | 0.25 | 1.16 | 1.28 | −0.12 | −0.34 | −0.80 | −2.08 | −2.21 | −0.13 | −0.07 | −0.15 |
| CuO/Ag(111) | 1.00 | 0.00 | 1.12 | 1.10 | 0.02 | 0.12 | −1.34 | −1.29 | −2.54 | −0.19 | −0.12 | 0.16 |
| $O^{sub}$(fcc)+CuO/Ag(111)[a] | 1.00 | 0.25 | 1.27 | 0.95 | 0.32 | −0.21 | −1.32 | −1.79 | −2.71 | −0.11 | −0.22 | 0.22 |
| $O^{sub}$(fcc)+CuO/Ag(111)[b] | 1.00 | 0.25 | 1.07 | 1.08 | −0.01 | −0.38 | −1.32 | −1.75 | −2.61 | −0.22 | −0.22 | 0.12 |
| $Cu_1Ag_3O$+CuO/Ag(111) | 1.25 | 0.25 | 1.36 | 1.04 | 0.32 | −0.52 | −1.52 | −2.03 | −2.85 | −0.10 | −0.35 | 0.25 |
| $Cu_2Ag_2O_2$+CuO/Ag(111) | 1.50 | 0.50 | | | | −0.77 | −1.76 | −2.25 | −3.07 | −0.19 | −0.16 | 0.28 |
| $Cu_3Ag_1O_2$+CuO/Ag(111) | 1.75 | 0.50 | | | | −0.63 | −1.75 | −2.11 | −3.07 | −0.16 | −0.16 | 0.07 |
| $Cu_4O_4$+CuO/Ag(111) | 2.00 | 1.00 | | | | −0.40 | −1.50 | −1.98 | −2.80 | −0.17 | −0.24 | 0.06 |

$2 \times 2$ cell) is necessary to promote the presence of $O^{sub}$. The calculations show that $O^{sub}$ atoms prefer to reside right at the interface under the first CuO layer rather than on the surface or deeper in the Ag slab (i.e., under the second Ag layer). This is due to the fact that the Cu−O bond is considerably stronger than the Ag−O one.[26]

From the phase diagram in Fig. 2 we can see that as the number of Cu atoms replacing Ag in the second layer increases, so does the number of $O^{sub}$ atoms at the interface. The surface free energy tends to decrease as more CuO layers are formed, in agreement with the fact that bulk CuO is stable phase at this value of oxygen chemical potential.[26,27]

### B. Effects of $O^{sub}$ and Cu content on activity and selectivity: NEB calculations

In this section we study the minimum energy paths (MEP) for the oxidation of ethylene along the two competing paths, leading to the formation of either Ac or EO. Linic and co-workers have experimentally shown the existence of a common OMC intermediate for both reaction paths on clean Ag.[20] In our simulations, the initial state is ethylene physisorbed at the catalyst surface and in all cases we find the reaction to go through an OMC intermediate before branching to give one of the two products. On each surface structure we identified several OMC geometries, often with similar energetics (see Table I).

Given the common OMC intermediate, within transition state theory (assuming the pre-exponential factors to be the same) the selectivity towards the formation of EO is a function of the difference in the activation energy for the two competing processes. We therefore define $\Delta E^* = E^*_{Ac} - E^*_{EO}$, and positive values of $\Delta E^*$ indicate that the formation of EO is kinetically, albeit not thermodynamically, favored.

The energies of local minima and transition states along the minimum energy paths computed through NEB calculations are shown in Fig. 3. We considered six kinds of structures: Ag(111) in the absence and presence of $O^{sub}$, CuO/Ag(111) with and without one $O^{sub}$ atom, and $Cu_1Ag_3O$ + CuO/Ag(111), where one Cu atoms substitutes for Ag in the first layer of the Ag slab below the CuO layer. The values of the activation energies are reported in Table I. The results suggest that, on Ag(111), the presence of $O^{sub}$ increases the height of activation energies in both reactions (∼0.5 eV), in agreement with the results of Greeley and Mavrikakis.[43] On the thin oxide-like layer structures, on the other hand, $O^{sub}$ slightly decreases the activation energies, by ∼−0.05 eV. The behavior towards an increase of the Cu content, however, is different for two reaction paths: $E^*_{Ac}$ increases by 0.3 eV, while $E^*_{EO}$ is almost unchanged (∼−0.05 eV) as one Cu substitutes for Ag. This data seem to indicate that $O^{sub}$ can either increase or decrease the selectivity towards EO depending on the surface structure: its effect is detrimental in the case of Ag(111) while it can be beneficial in the case of CuO/Ag(111). The presence of Cu, on the other hand, clearly enhances the tendency to form EO, since the least selective among the Cu-containing structures ($\Delta E^* = -0.01$ eV) is more selective than the best Cu-free structure ($\Delta E^* = -0.08$ eV).

### C. Selectivity and activity indicators

In Fig. 4, we show the geometry of the transition state (TS) for the formation of both EO and Ac on the six surface structures discussed in Sec. III B. We can see, as already noticed by Kokalj *et al.*,[30] that the geometry of TS is not strongly influenced by the underlying catalyst surface. The TS of the OMC → EO reaction is characterized by a fully broken C-surface bond, while in the OMC → Ac case, at the TS both the C-surface and O-surface bonds are partially broken. On the basis of this observation, Kokalj *et al.*[30] decomposed the OMC-surface interaction into the sum of the interactions of methyl ($CH_3$•) and methoxy ($CH_3O$•) radicals with the surface. Accordingly, the authors postulated the activation energy of the two processes to depend linearly not only on the enthalpy of reaction (Brønsted-Evans-Polany principle), but also on the strength of the two radical-surface bonds according to:

$$E^{*(SI)}_{EO} = C_1 + \alpha_1 E^b_{CH_3} + \gamma E^{BEP}_{EO}, \quad (3)$$

$$E^{*(SI)}_{Ac} = C_2 + \alpha_2 E^b_{CH_3} + \beta E^b_{CH_3O} + \gamma E^{BEP}_{Ac}, \quad (4)$$

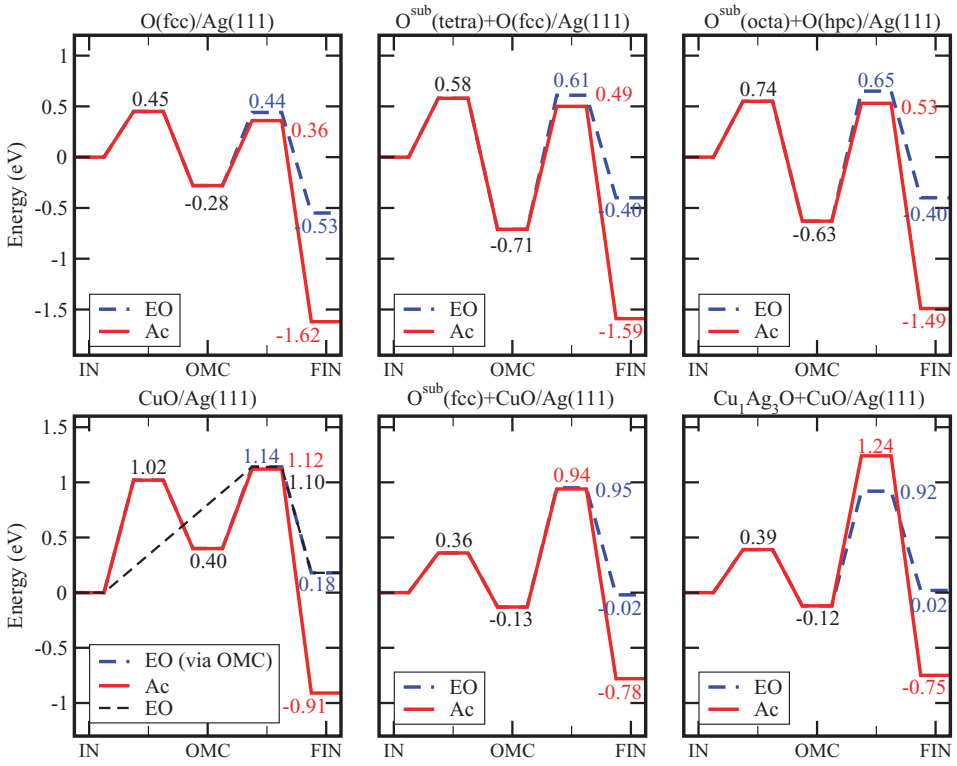


FIG. 3. Energy profiles for ethylene epoxidation over the selected surface structures. At the initial state (IN) ethylene is physisorbed on the surface, the intermediate state is the oxametallacycle (OMC), while the final state (FIN) of the reaction is either acetaldehyde (Ac, red solid line) or ethylene oxide (EO, blue dashed line) physisorbed on the surface. In the case of CuO/Ag(111), the formation of EO can proceed directly from the initial state without involving the OMC intermediate (black dashed line).

where

$$E_{\mathrm{Ac}}^{\mathrm{BEP}} = E_{\mathrm{Ac}}^{\mathrm{b}} - E_{\mathrm{OMC}}^{\mathrm{b}}, \tag{5}$$

$$E_{\mathrm{EO}}^{\mathrm{BEP}} = E_{\mathrm{EO}}^{\mathrm{b}} - E_{\mathrm{OMC}}^{\mathrm{b}}, \tag{6}$$

and $C_1$ and $C_2$ are two additive constants. The (SI) superscript is used to distinguish these quantities obtained with a "Selectivity Indicator" from those computed directly through a NEB calculation.

The selectivity towards the formation of EO is a function of $\Delta E^* = E_{\mathrm{Ac}}^* - E_{\mathrm{EO}}^*$, which therefore reads:

$$\Delta E^{*(\mathrm{SI})} = \alpha E_{\mathrm{CH_3}}^{\mathrm{b}} + \beta E_{\mathrm{CH_3O}}^{\mathrm{b}} + \gamma\left[E_{\mathrm{Ac}}^{\mathrm{b}} - E_{\mathrm{EO}}^{\mathrm{b}}\right] + C, \tag{7}$$

with $\alpha = \alpha_2 - \alpha_1$. Fitting $C$, $\alpha$, $\beta$, and $\gamma$ against a series of NEB calculations on clean metal surfaces (Ag, Cu, Rh, and Au), Kokalj *et al.*[30] obtained $\alpha \simeq -\beta \simeq \gamma = 0.39$ eV. This selectivity indicator could fit their data set with a root-mean-square-error (RMSE) of 0.05 eV and a maximum-absolute-error (MAE) of 0.07 eV. We tested the

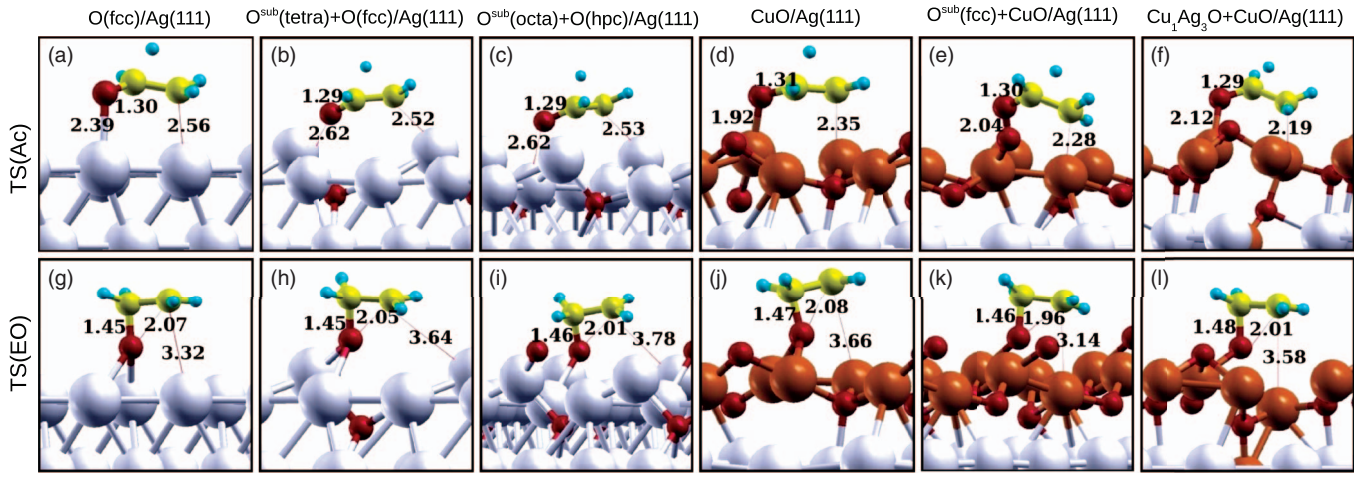


FIG. 4. Transition state geometries for the formation of acetaldehyde (a)–(f) and ethylene oxide (g)–(l) for the six low energy structures considered in this work. The red, brown, gray, yellow, and green spheres represent O, Cu, Ag, C, and H atoms, respectively.

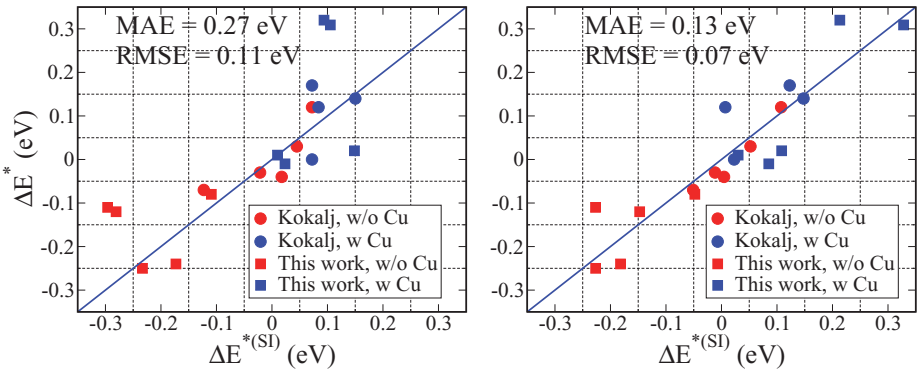


FIG. 5. Comparison of the ability of two selectivity indicators to predict the difference in activation energy for the two reaction paths considered. $\Delta E^*$ are the values obtained through NEB calculations, $\Delta E^{*(SI)}$ are those obtained using the selectivity indicators. Left panel: selectivity indicator proposed by Kokalj *et al.*[30] Right panel: selectivity indicator obtained by refitting the parameters of Kokalj's indicator. Circles represent the data set used by Kokalj *et al.*,[30] squares the structures computed in this work. Red symbols indicate Cu-free structures, blue symbols Cu-containing structures.

applicability of this indicator on our set of structures, comprising both clean Ag(111) and CuO/Ag(111), with and without subsurface oxygen, as well as $Cu_xAg_yO$ + CuO/Ag(111) structures and found a much poorer agreement with the NEB results, leading to RMSE = 0.11 eV and MAE = 0.27 eV.

To derive an indicator able to describe the selectivity both on clean metal surfaces as well as on structures covered with thin CuO layers, we first refitted the parameters of the selectivity indicator proposed by Kokalj *et al*. The data set for the fitting includes all the structures described in Table I (squares in Fig. 5) as well as the structures originally used in the derivation of the selectivity indicator[30] (circles in Fig. 5). Keeping $\alpha = -\beta$, we obtain values of 0.24, 1.01, and −0.12 for $\alpha$, $\gamma$, and $C$, respectively, leading to RMSE = 0.07 eV and MAE = 0.13 eV (see Fig. 5). The fact that the largest coefficient in this linear fit is $\gamma$ suggests that the difference in binding energy between the final products plays the largest role, as predicted by the BEP principle. As can be seen in Table I, however, these quantities do not vary appreciably from structure to structure, while the binding energies of the methyl and methoxy radical strongly depend on the catalyst surface.

The data shown in Fig. 5 clearly show that the structures containing Cu (blue circles and squares) tend to have a higher selectivity towards EO compared to Cu-free structures (red circles and squares), given the fact that most of the blue symbols are found on the top right corner of the graph. The selectivity indicator correctly captures the improvement in selectivity of Cu-containing structures, thus showing that this effect is to be attributed to the ability of Cu to increase the strength of the O-surface bond compared to the C-surface bond. This is in agreement with the results presented by Kokalj *et al*. on metal surfaces.[30] We cannot fail to notice, however, that the error in the selectivity indicator (∼0.1 eV) is often as big as the differences in $\Delta E^*$ between one structure and the other. Its quantitative predictive power is limited in the cases where $\Delta E^* \lesssim 0.1$ eV. It allows, however, to rationalize the reason for the improvement in selectivity of Ag-Cu alloys compared to pure Ag on the basis of the relative strength of bonds between OMC and the surface.

To get further insights into the role of Cu in improving the selectivity of Ag, we separately fitted the parameters of Eqs. (3) and (4), obtaining the following expressions for the indicators of the activity towards EO and Ac:

$$E_{EO}^{*(SI)} = -0.08E_{CH_3}^{b} + 0.45E_{EO}^{b} - 0.68E_{OMC}^{b} + 1.24\,\text{eV}, \quad (8)$$

$$E_{Ac}^{*(SI)} = 0.02E_{CH_3}^{b} + 0.01E_{CH_3O}^{b} + 0.57E_{Ac}^{b} - 0.87E_{OMC}^{b} + 0.98\,\text{eV}. \quad (9)$$

The quality of the fit is shown in Fig. 6. We obtain a RMSE of 0.09 eV and MAE of 0.23 eV for $E_{Ac}^*$ and a RMSE

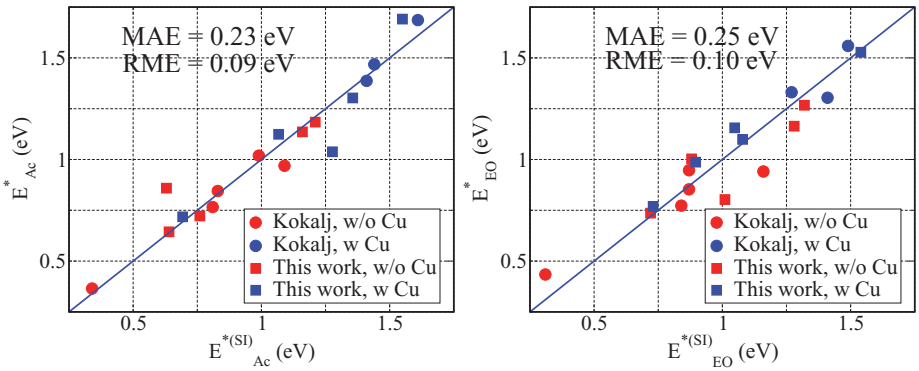


FIG. 6. Activation energies for the formation for Ac (left panel) and EO (right panel) obtained from NEB calculations ($E^*$), and from the indicators in Eqs. (3) and (4), ($E^{*(SI)}$). The meaning of the symbols is the same as in Fig. 5.

of 0.10 eV and a MAE of 0.25 eV for $E^{*}_{EO}$. Comparing the two panels in Fig. 6 we can see that while the presence of Cu tends to increase the activation energy towards the formation of Ac, no such effect is present for the selective path. The overall effect of Cu, through an increase of the metal-oxygen bond relative to the metal carbon bond, is therefore to suppress the unselective reaction channel.

A closer look at Eqs. (8) and (9) reveals that the activity of the catalyst mostly depends on the binding energy of the OMC intermediate, since the largest coefficient in both expressions is the one in form of $E^{b}_{OMC}$. As we can see from the data reported in Table I, this quantity changes appreciably from structure to structure, giving rise to variations in the activation energies of a factor of 2. To improve the activity of the CuO/Ag catalyst, while keeping its high selectivity, one should therefore aim at decreasing the stability of the OMC intermediate. This suggests a possible strategy in the search for superior alloy catalysts for ethylene epoxidation.

## IV. CONCLUSIONS

Using DFT calculations we studied the catalytic properties of Ag-Cu alloys for ethylene epoxidation, accounting for the fact that Cu tends to oxidize and form thin Cu-oxide layers on top of the Ag particles. We investigated the role played by subsurface oxygen and found that, depending on the catalyst surface structure, it can either increase or decrease the selectivity towards the formation of ethylene oxide. The thermodynamic stability of subsurface oxygen is enhanced in the presence of high Cu contents, in line with the fact that the formation of bulk Cu-oxide is favored at values of temperature and pressure typically used in ethylene epoxidation.

By reparametrizing the indicator proposed by Kokalj *et al.*,[30] we developed indicators of the catalysts activity and selectivity based on binding energies of reactants, intermediates, and products which estimate barrier heights and differences in barriers with errors of the order of ≈0.1 eV. As shown earlier for clean metal surfaces, we find that the improved selectivity of CuO layers on Ag is due to an increase of the strength of the surface-oxygen bond relative to the surface carbon bond. The activity of the catalyst, on the other hand, is mainly due to the strength of the interaction between the OMC intermediate and the surface. Reducing OMC binding energy while at the same time retaining the high selectivity afforded by CuO layers might constitute a rational strategy to design improved alloy catalysts for ethylene epoxidation.

## ACKNOWLEDGMENTS

We acknowledge generous computer time allocations at CINECA (Grant No. SubEPOXY - HP10BS8TNM) and at Caspur (Standard HPC Grant 2011).

[1]B. K. Hodnett, *Heterogeneous Catalytic Oxidation: Fundamental and Technological Aspects of the Selective and Total Oxidation of Organic Compounds* (John Wiley, New York, 2000).
[2]Global CCS Institute, CCS Roadmap for Industry, see http://www.globalccsinstitute.com.
[3]K. Weissermel and H. Arpe, *Industrial Organic Chemistry* (Wiley-VCH, Weinheim, 1993).
[4]Shell, Ethylene oxide/ethylene glycol (EO/EG) processes, see http://www.shell.com/global/products-services/solutions-for-businesses/globalsolutions/refinery-chemical-licensing/petrochemical-technology/ethylene-oxide-processes.html, accessed January 2013.
[5]C. T. Campbell and M. T. Paffett, Surf. Sci. **139**, 396 (1984).
[6]C. T. Campbell, J. Catal. **94**, 436 (1985).
[7]R. Grant and R. Lambert, J. Catal. **92**, 364 (1985).
[8]R. V. Santen and C. de Groot, J. Catal. **98**, 530 (1986).
[9]P. J. van den Hoek, E. J. Baerends, and R. van Santen, J. Phys. Chem. **93**, 6469 (1989).
[10]M. Rocca, L. Savio, L. Vattuone, U. Burghaus, V. Palomba, N. Novelli, F. Buatier de Mongeot, U. Valbusa, R. Gunnella, G. Comelli, A. Baraldi, S. Lizzit, and G. Paolucci, Phys. Rev. B **61**, 213 (2000).
[11]L. Savio, L. Vattuone, M. Rocca, F. B. de Mongeot, G. Comelli, A. Baraldi, S. Lizzit, and G. Paolucci, Surf. Sci. **506**, 213 (2002).
[12]V. I. Bukhtiyarov, M. Hävecker, V. V. Kaichev, A. Knop-Gericke, R. W. Mayer, and R. Schlögl, Phys. Rev. B **67**, 235422 (2003).
[13]T. C. R. Rocha, A. Oestereich, D. V. Demidov, M. Havecker, S. Zafeiratos, G. Weinberg, V. I. Bukhtiyarov, A. Knop-Gericke, and R. Schlogl, Phys. Chem. Chem. Phys. **14**, 4554 (2012).
[14]M. Ozbek, I. Onal, and R. van Saten, J. Catal. **284**, 230 (2011).
[15]M. O. Ozbek, I. Onal, and R. A. van Santen, ChemCatChem **3**, 150 (2011).
[16]J. Schnadt, J. Knudsen, X. L. Hu, A. Michaelides, R. T. Vang, K. Reuter, Z. Li, E. Lægsgaard, M. Scheffler, and F. Besenbacher, Phys. Rev. B **80**, 075424 (2009).
[17]D. S. Su, T. Jacob, T. Hansen, D. Wang, R. Schlgl, B. Freitag, and S. Kujawa, Angew. Chem., Int. Ed. **47**, 5005 (2008), ISSN 1521–3773.
[18]W.-X. Li, C. Stampfl, and M. Scheffler, Phys. Rev. B **65**, 075407 (2002).
[19]W.-X. Li, C. Stampfl, and M. Scheffler, Phys. Rev. B **67**, 045408 (2003).
[20]S. Linic and M. A. Barteau, J. Am. Chem. Soc. **124**, 310 (2002).
[21]S. Linic and M. A. Barteau, J. Am. Chem. Soc. **125**, 4034 (2003).
[22]D. Torres, N. Lopez, F. Illas, and R. M. Lambert, J. Am. Chem. Soc. **127**, 10774 (2005).
[23]M. Ozbek, I. Onal, and R. Santen, Top. Catal. **55**, 710 (2012).
[24]S. Linic, J. T. Jankowiak, and M. A. Barteau, J. Catal. **224**, 489 (2004).
[25]S. Piccinin, S. Zafeiratos, C. Stampfl, T. Hansen, M. Havecker, D. Teschner, V. Bukhtiyarov, F. Girgsdies, A. Knop-Gericke, R. Schlöegl, and M. Scheffler, Phys. Rev. Lett. **104**, 035503 (2010).
[26]S. Piccinin, C. Stampfl, and M. Scheffler, Phys. Rev. B **77**, 075426 (2008).
[27]S. Piccinin, C. Stampfl, and M. Scheffler, Surf. Sci. **603**, 1467 (2009).
[28]S. Piccinin, N. L. Nguyen, C. Stampfl, and M. Scheffler, J. Mater. Chem. **20**, 10521 (2010).
[29]N. L. Nguyen, S. Piccinin, and S. de Gironcoli, J. Chem. Phys. C **115**, 10073 (2011).
[30]A. Kokalj, P. Gava, S. de Gironcoli, and S. Baroni, J. Catal. **254**, 304 (2008).
[31]J. Perdew, K. Burke, and M. Ernzerhof, Phys. Rev. Lett. **77**, 3865 (1996).
[32]D. Vanderbilt, Phys. Rev. B **41**, 7892 (1990).
[33]The ultrasolft pseudopotentials for Ag, Cu, O, C, and H were taken from QUANTUM-ESPRESSO pseudopotential download page, see http://www.quantum-espresso.org (files: Ag.pbe-d-rrkjus.UPF, Cu.pbe-d-rrkjus.UPF, O.pbe-rrkjus.UPF, C.pbe-rrkjus.UPF, and H.pbe-rrkjus.UPF).
[34]H. J. Monkhorst and J. D. Pack, Phys. Rev. B **13**, 5188 (1976).
[35]N. Marzari, D. Vanderbilt, A. D. Vita, and M. C. Payne, Phys. Rev. Lett. **82**, 3296 (1999).
[36]G. Henkelman, B. P. Uberuaga, and H. Johnson, J. Chem. Phys. **113**, 9901 (2000).
[37]P. Giannozzi *et al.*, J. Phys.: Condens. Matter **21**, 395502 (2009).
[38]C. Stampfl, Catal. Today **105**, 17 (2005).
[39]K. Reuter and M. Scheffler, Phys. Rev. B **65**, 035406 (2001).
[40]S. Zafeiratos, S. Piccinin, and D. Teschner, Catal. Sci. Technol. **2**, 1787 (2012).
[41]J. Kim, J. Rodriguez, J. Hanson, A. Frenkel, and P. Lee, J. Am. Chem. Soc. **125**, 10684 (2003).
[42]Y. Xu, J. Greeley, and M. Marvrikakis, J. Am. Chem. Soc. **127**, 12823 (2005).
[43]J. Greeley and M. Mavrikakis, J. Phys. Chem. C **111**, 7992 (2007).
[44]C. Backx, J. Moolhuysen, P. Geenen, and R. van Santen, J. Catal. **72**, 364 (1981).
[45]M. Atkins, J. Couves, M. Hague, B. Sakakini, and K. Waugh, J. Catal. **235**, 103 (2005).

[46]M. Dean, A. McKee, and M. Bowker, Surf. Sci. **211**, 1061 (1989).
[47]A. Kleyn, D. Butler, and A. Raukema, Surf. Sci. **363**, 29 (1996).
[48]X. Bao, M. Muhler, T. Schedel-Niedrig, and R. Schlögl, Phys. Rev. B **54**, 2249 (1996).
[49]A. Y. Lozovoi, A. Alavi, and M. W. Finnis, Phys. Rev. Lett. **85**, 610 (2000).
[50]K. Reuter, M. V. Ganduglia-Pirovano, C. Stampfl, and M. Scheffler, Phys. Rev. B **65**, 165403 (2002).
[51]M. Ganduglia-Pirovano, K. Reuter, and M. Scheffler, Phys. Rev. B **65**, 245426 (2002).
[52]M.-L. Bocquet, P. Sautet, J. Cerda, C. I. Carlisle, M. J. Webb, and D. A. King, J. Am. Chem. Soc. **125**, 3119 (2003).